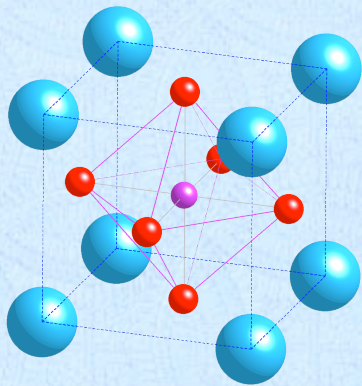
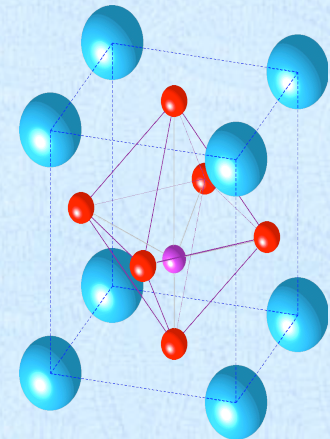


In situ polarization dynamics and atomic structure of ultrathin oxides



Arthur P. Baddorf



**Junsoo Shin
Von Braun Nascimento
E. Ward Plummer
Sergei V. Kalinin
Peter Maksymovych**

The Message



Even “inert” oxides react in air



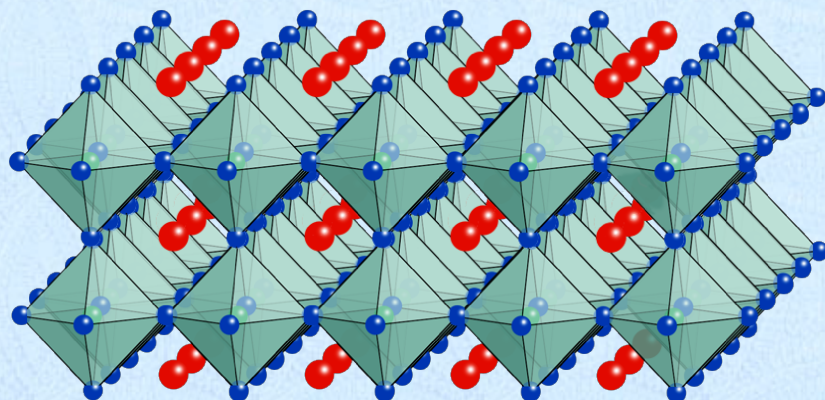
Ultrathin ferroelectricity depends on the surface



PFM is different in air and vacuum



SrRuO₃ Thin Films



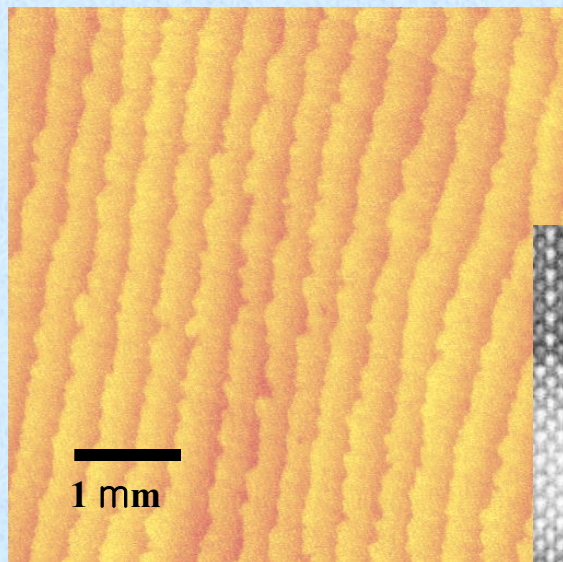
● Sr ● O ● Ru (center of octahedra)



- **Ferromagnetic metal**
- **Perovskite oxide – with good transport properties**
- **Electrode for oxide based devices**

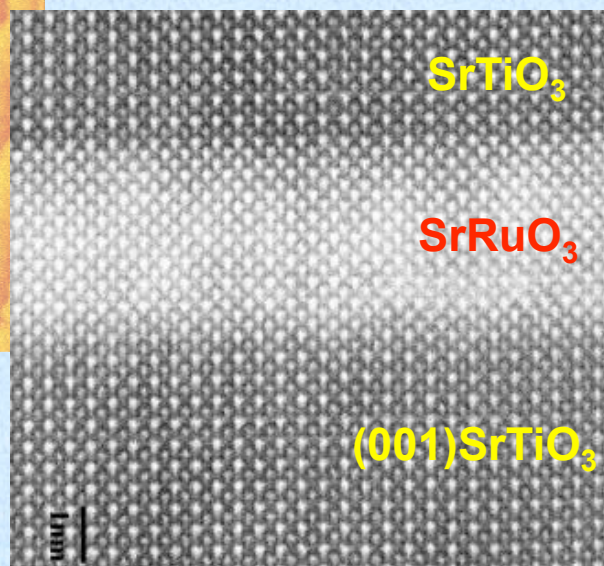
SrRuO₃: The Ideal Oxide Electrode

ambient AFM



4nm thick SrRuO₃ film

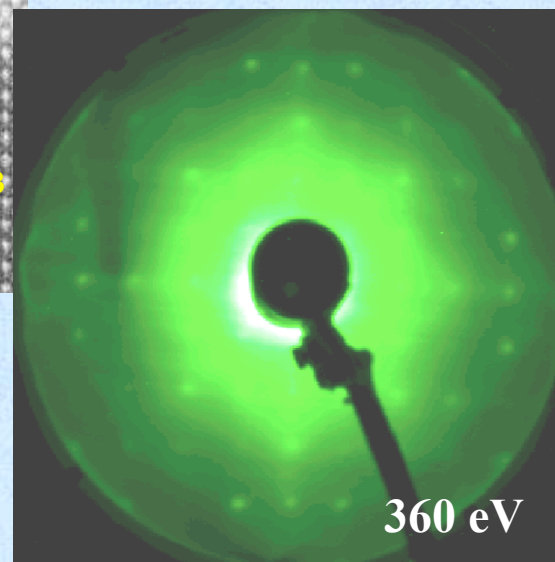
cross-sectional STEM



STEM by M. F. Chisholm (ORNL)

J. Shin, S. V. Kalinin, H. N. Lee, H. M. Christen, R. G. Moore, E. W. Plummer, and A. P. Baddorf *J. Mater. Res.* (2004)

electron diffraction

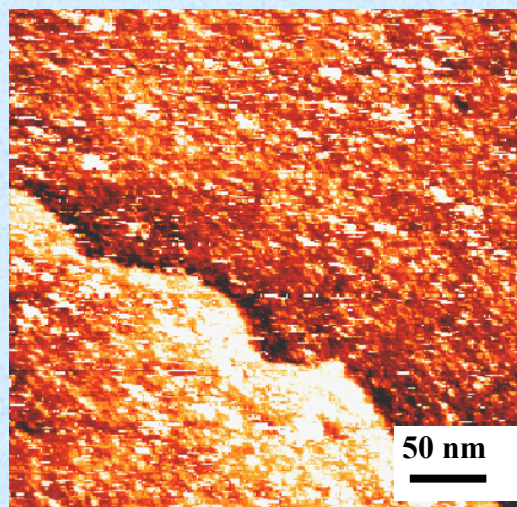


- **Extremely flat, single steps**
- **Highly crystalline**
- **Chemically stable, even after exposure to air**

SrRuO₃: An Abysmal Failure

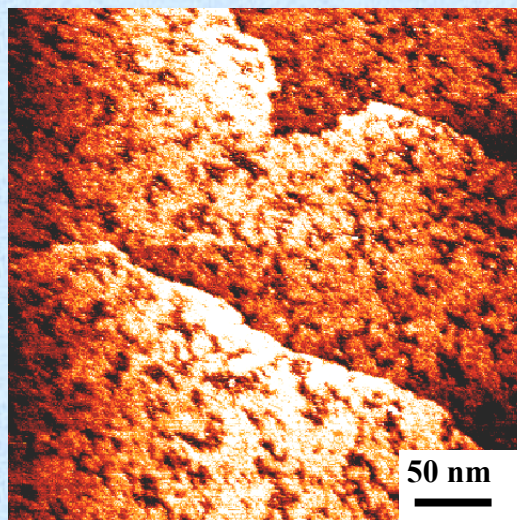
STM images at RT

annealing temperature
RT

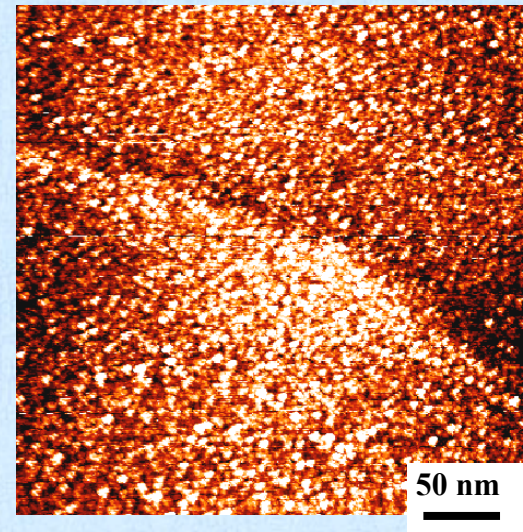


Exposed to air then annealed in vacuum

300°C



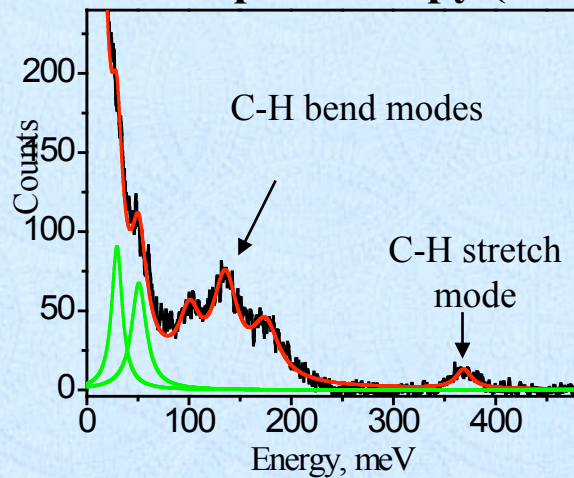
800°C



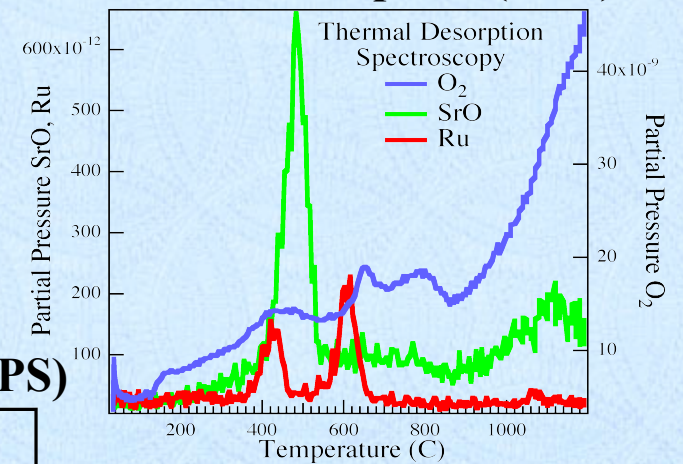
- Surface falls apart after gentle anneal

The Culprit: Air Exposure

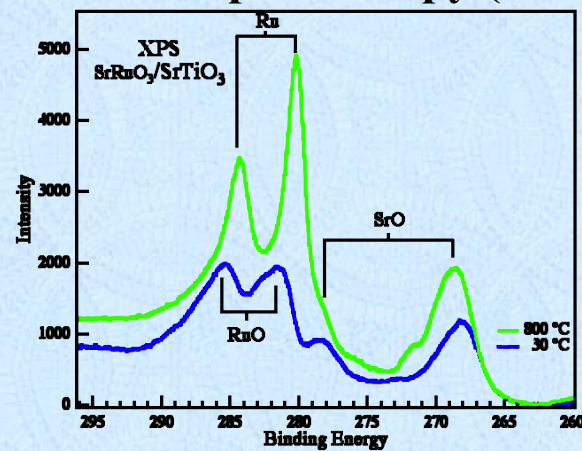
vibrational spectroscopy (HREELS)



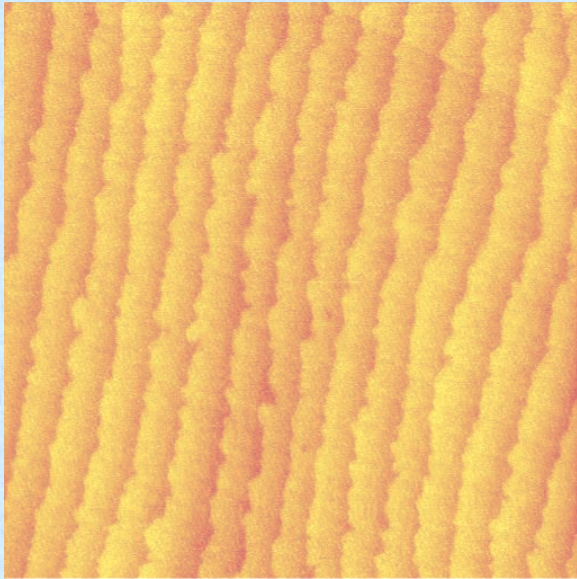
thermal desorption (TDS)



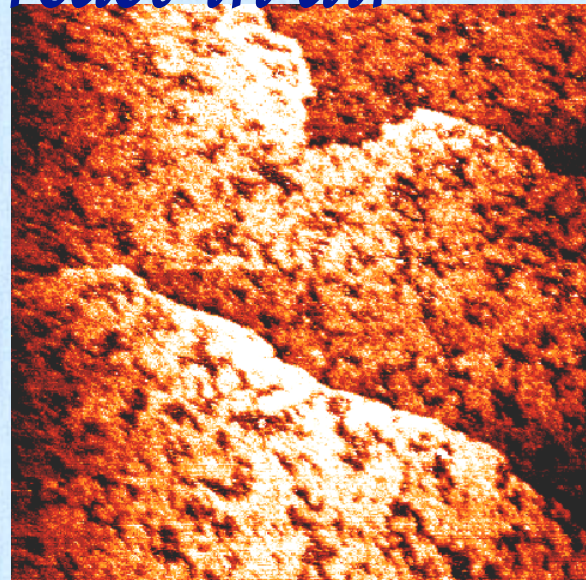
electron spectroscopy (XPS)

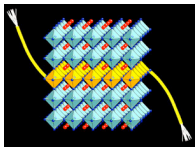


- Adsorbed hydrocarbons react with the surface
- Metallic Ru and oxide Sr remain



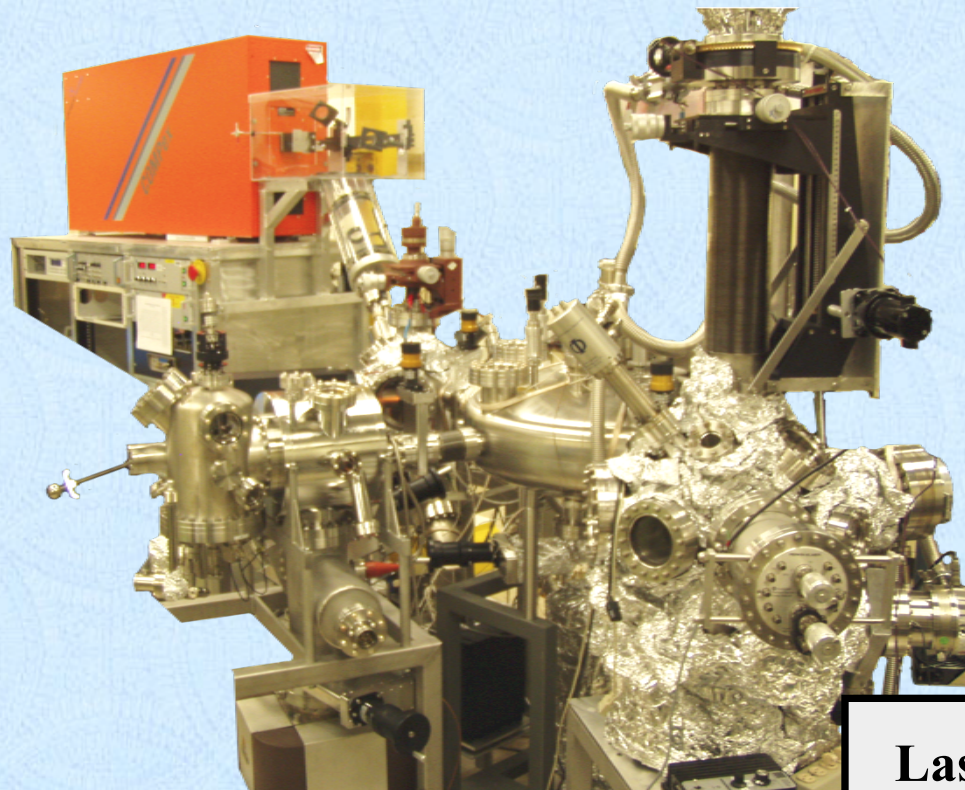
Even “inert” oxides react in air



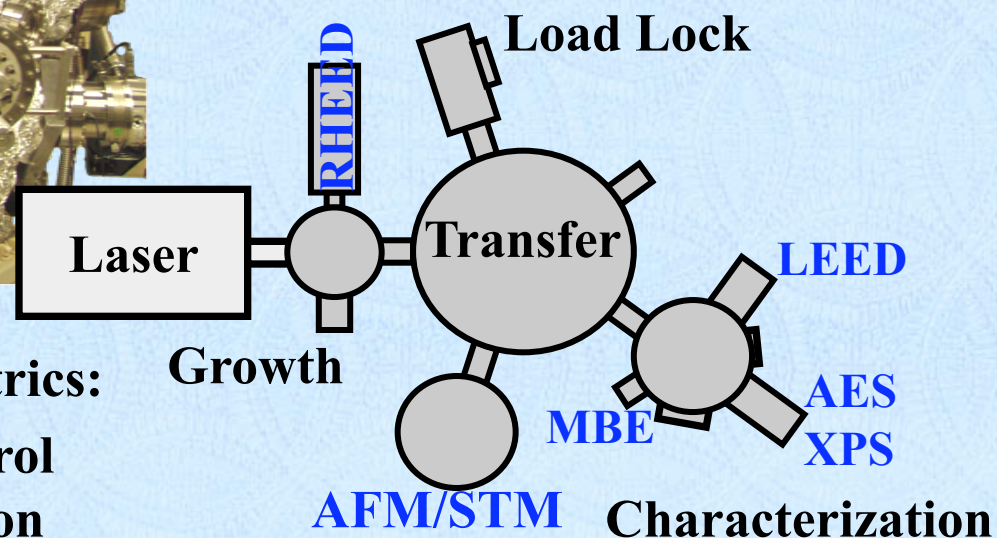


NanoTransport System

In-situ Growth and Characterization of Oxide Films



PLD growth
Electron Diffraction
Electron Spectroscopy
LEED-IV structure
VT STM/AFM

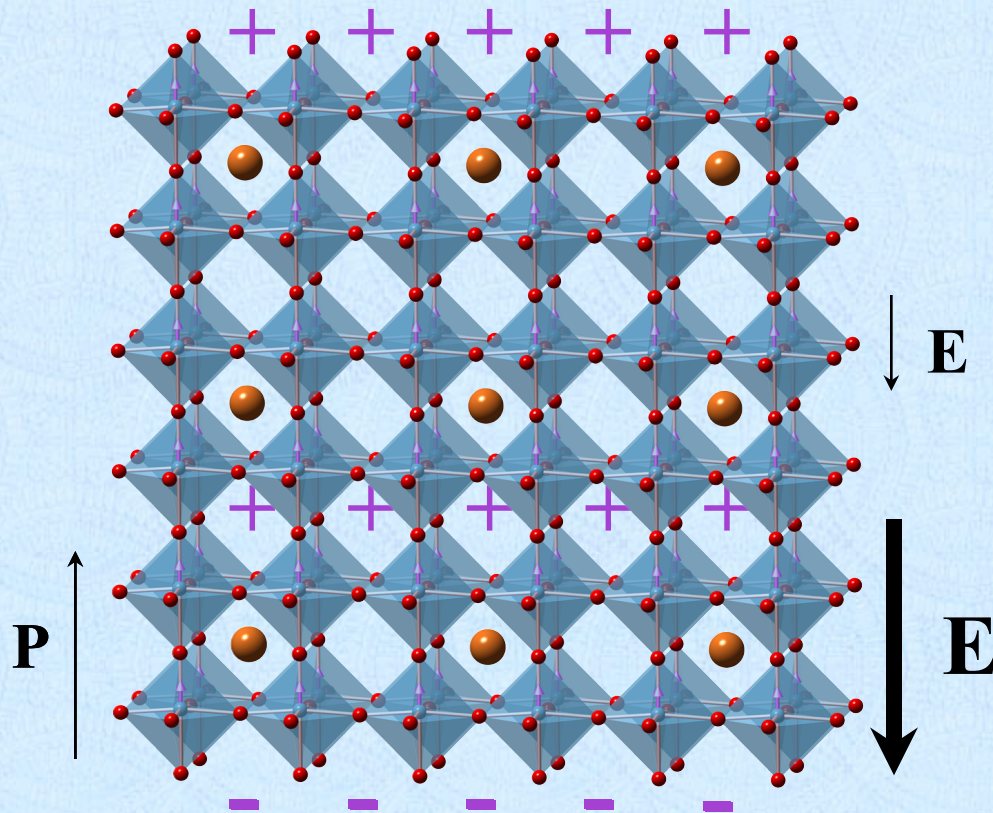


Advantages for ultrathin ferroelectrics:

- ❖ high degree of control
- ❖ avoids contamination
- ❖ no top layer metal interface
- ❖ no pin hole/defect complications

Ultrathin Ferroelectric Films

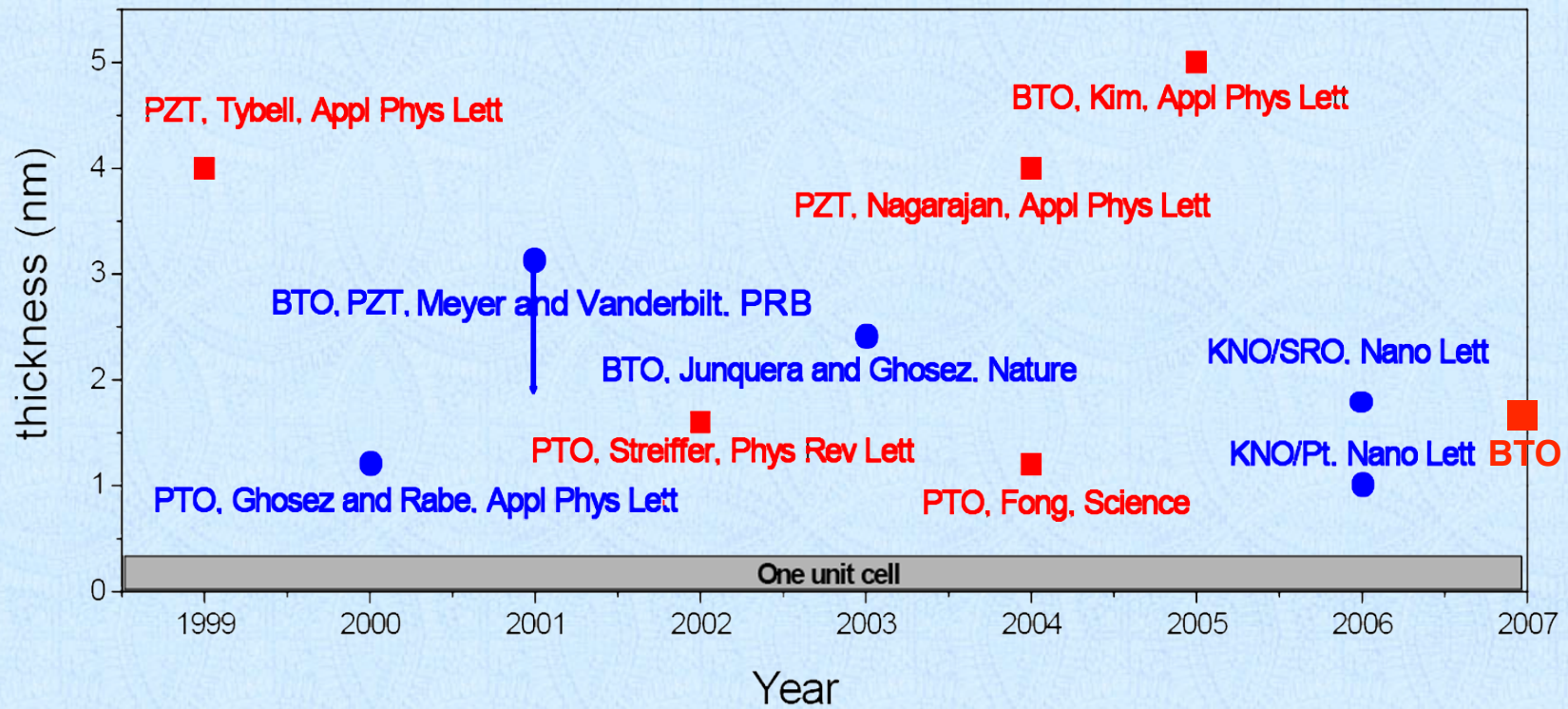
Ferroelectrics couple structure and electrical field

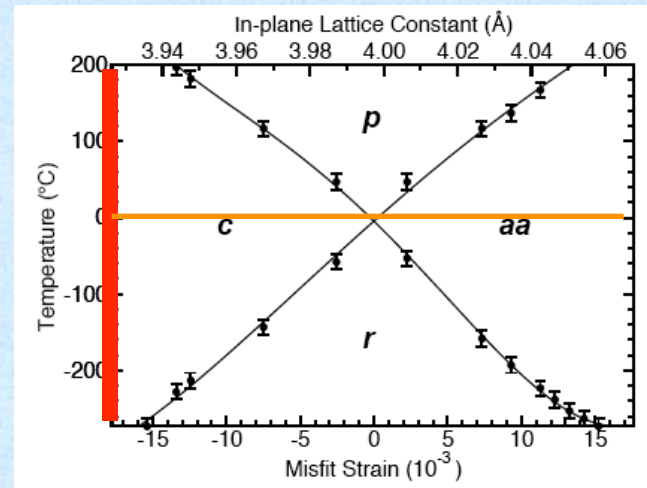


- ❖ spontaneous polarization
- ❖ voltage controlled motion
- ❖ high dielectric response
- ❖ nonvolatile memory

Depolarizing field may limit thinness

Minimum Ferroelectric Film Thickness





p none
aa in-plane
r diagonal
c z

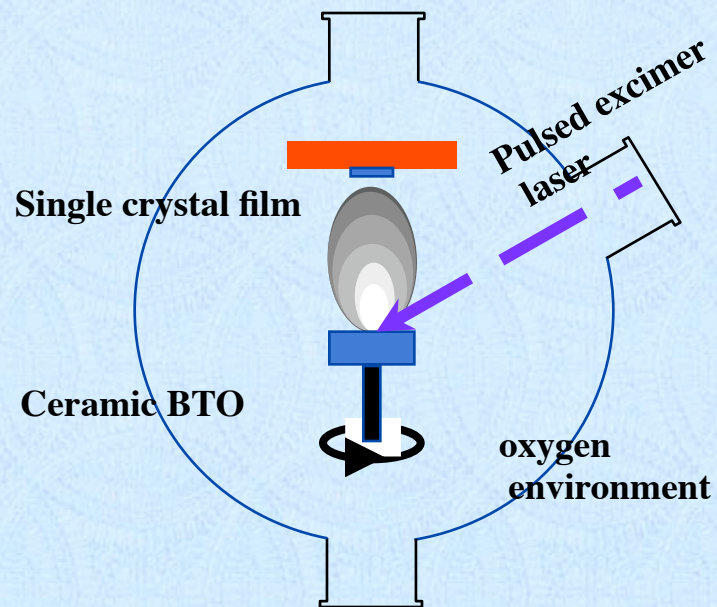
Diéguez, ... Rabe, Vanderbilt PRL04

Strain favors vertical polarization over wide range of temperature

growth

Film Growth

Film growth by pulsed laser deposition



- ❖ high pressure O₂ (10-100 mTorr)
- ❖ high temperature (650-825 °C)
- ❖ UHV compatible

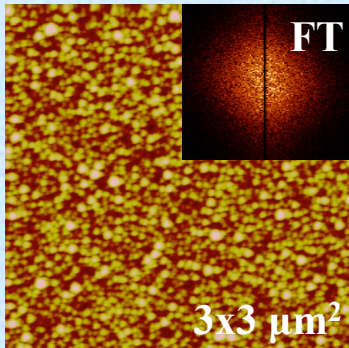
kinetically limited growth

Growth of BaTiO₃/SrTiO₃ using kinetic limitations

AFM

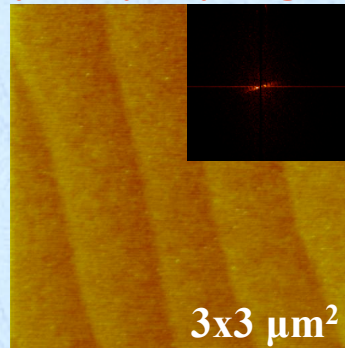
Junsoo Shin, A.Y. Borisevich, S.V. Kalinin, E.W. Plummer, and A.P. Baddorf, APL 2007 in print

3D island growth



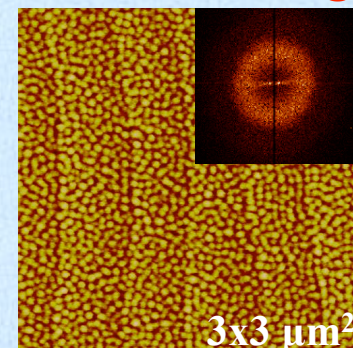
$P_{O_2} = 100 \text{ mTorr}$
 $T = 700 \text{ }^\circ\text{C}$
 $R = 0.2 \text{ ML/s}$

Layer-by-layer growth



$P_{O_2} = 10 \text{ mTorr}$
 $T = 650 \text{ }^\circ\text{C}$
 $R = 0.2 \text{ ML/s}$

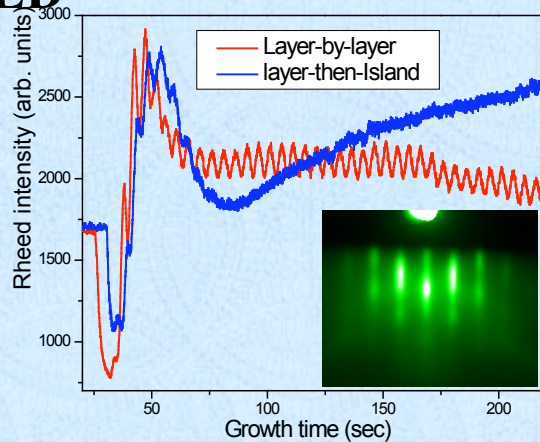
Pseudo 2D island growth



$P_{O_2} = 10 \text{ mTorr}$
 $T = 825 \text{ }^\circ\text{C}$
 $R = 0.2 \text{ ML/s}$

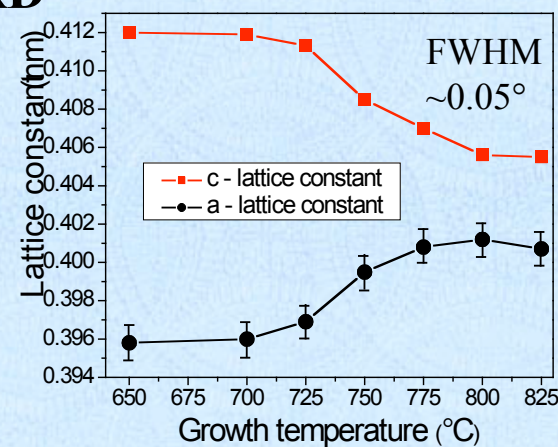
new growth mode

RHEED



layer-by-layer oscillations

XRD

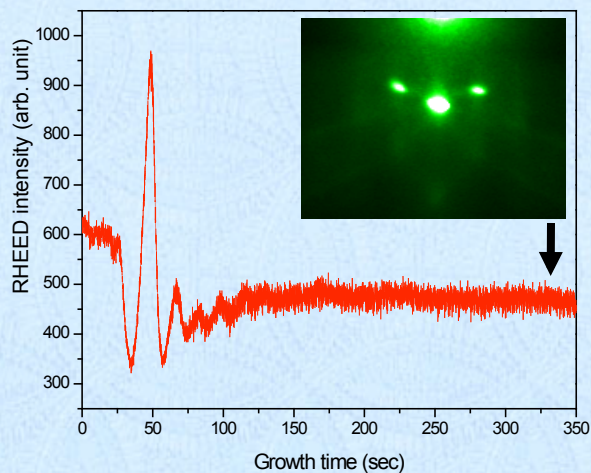


highly strained films

ex-situ characterization

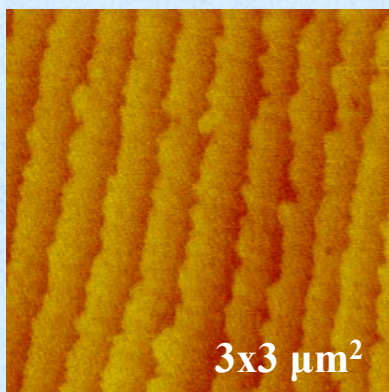
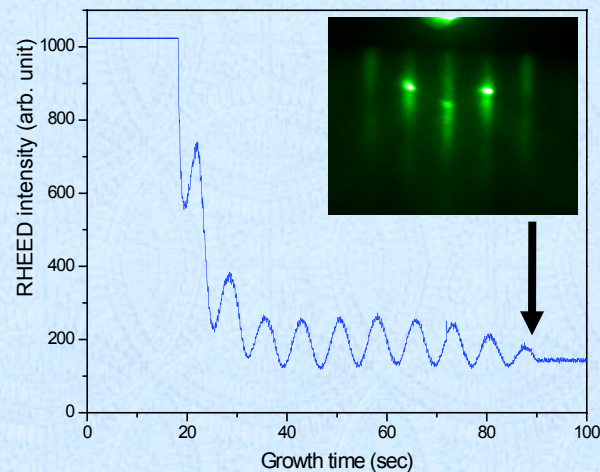
Ultra-thin BaTiO_3 with metallic electrode ($\text{BaTiO}_3/\text{SrRuO}_3/\text{SrTiO}_3$)

SrRuO_3
step flow growth

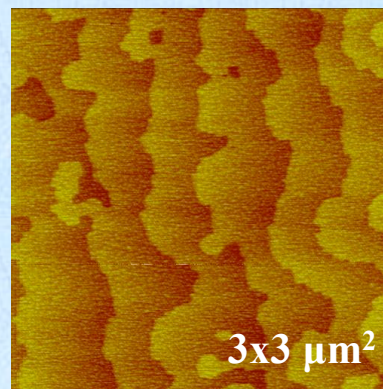


RHEED

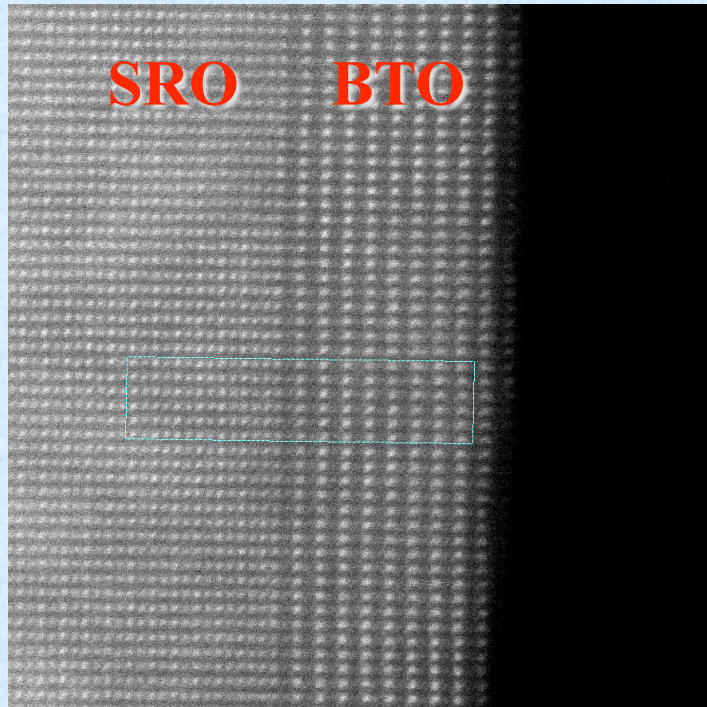
BaTiO_3
layer by layer growth



15 nm thick

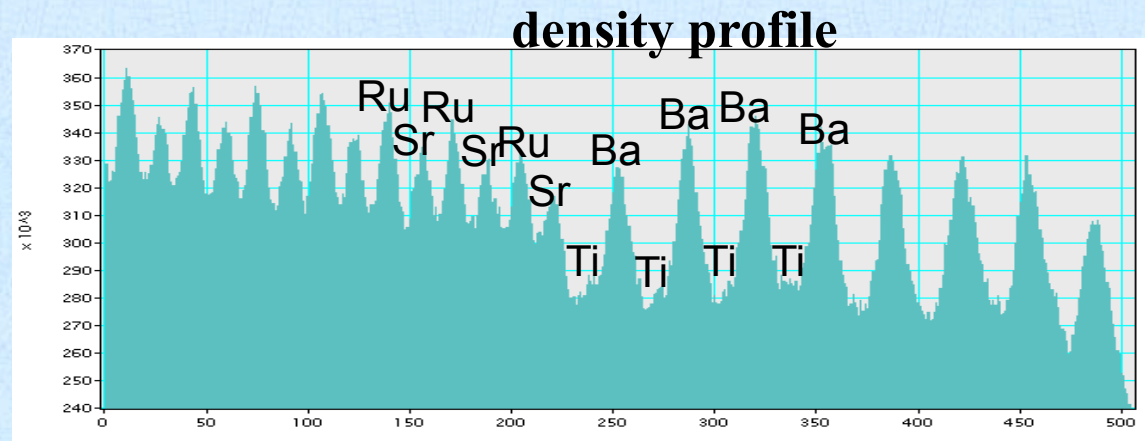


10 ML = 4.2 nm



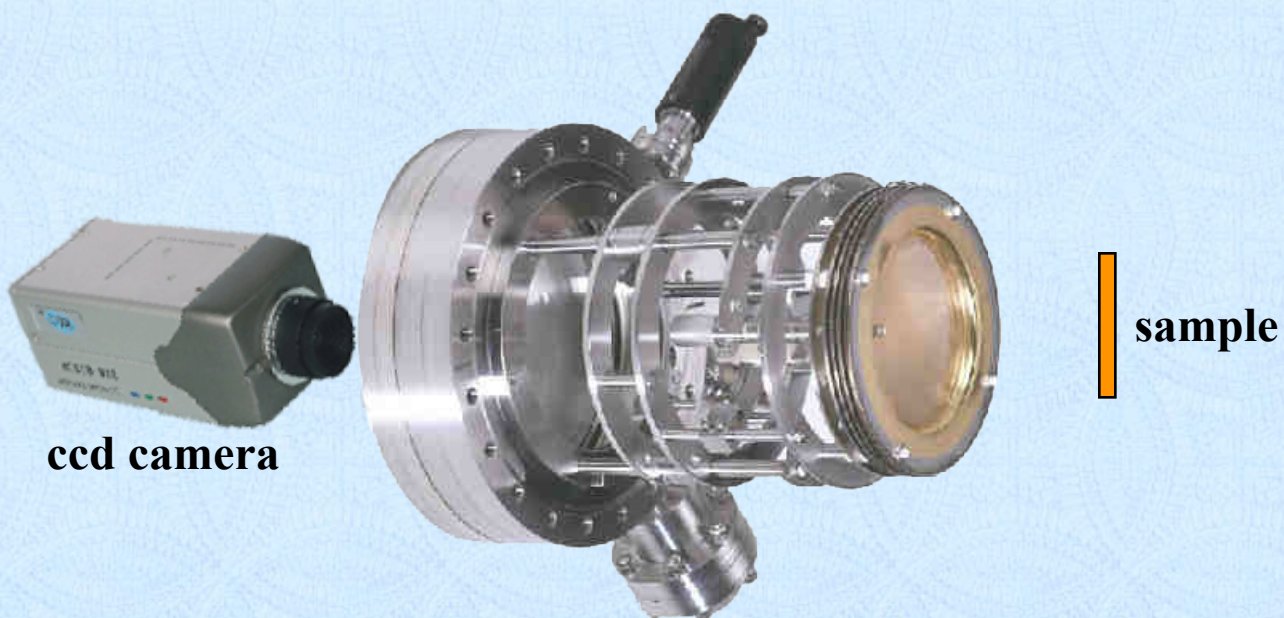
BaTiO₃ – SrRuO₃ Interface STEM

- ❖ crystalline
- ❖ clean interface
- ❖ possible mixing in one layer



structure

Low Energy Electron Diffraction LEED

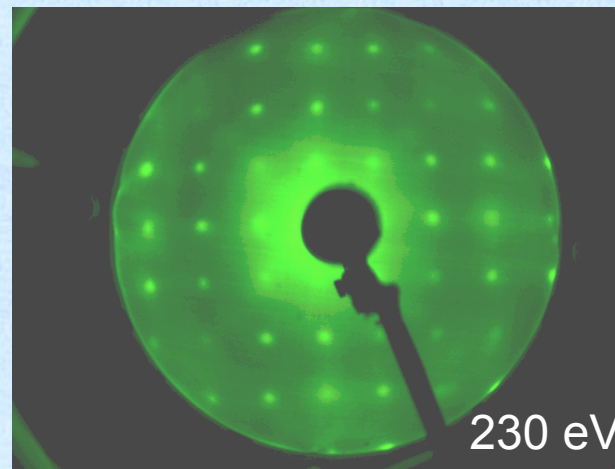
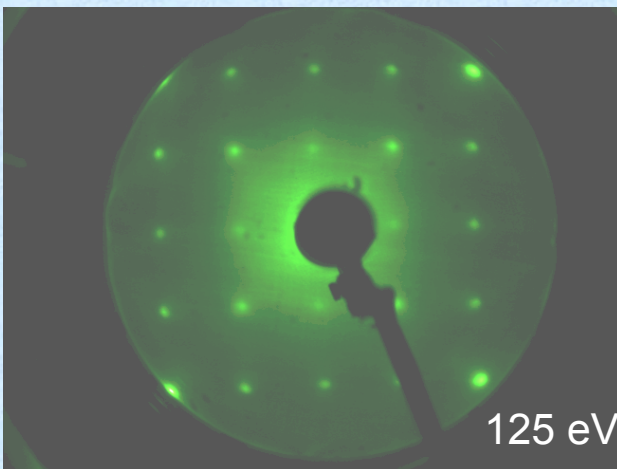
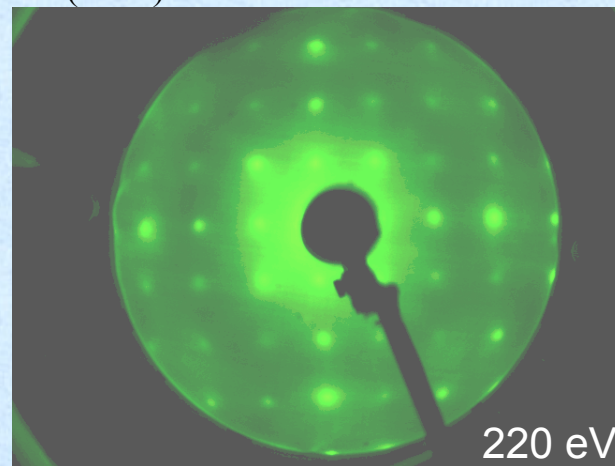
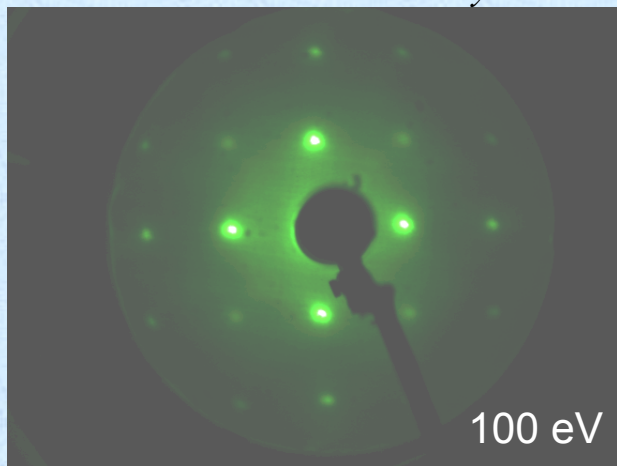


Low Energy Electron Diffraction

10 Layer BTO/SRO/STO

Junsoo Shin, V.B. Nascimento, A.Y. Borisevich, E.W. Plummer, S.V. Kalinin, and A.P. Baddorf

Phys. Rev. B 77, 245437 (2008)



- ❖ crystalline
- ❖ tetragonal

LEED-IV 10 Layer BaTiO₃ film

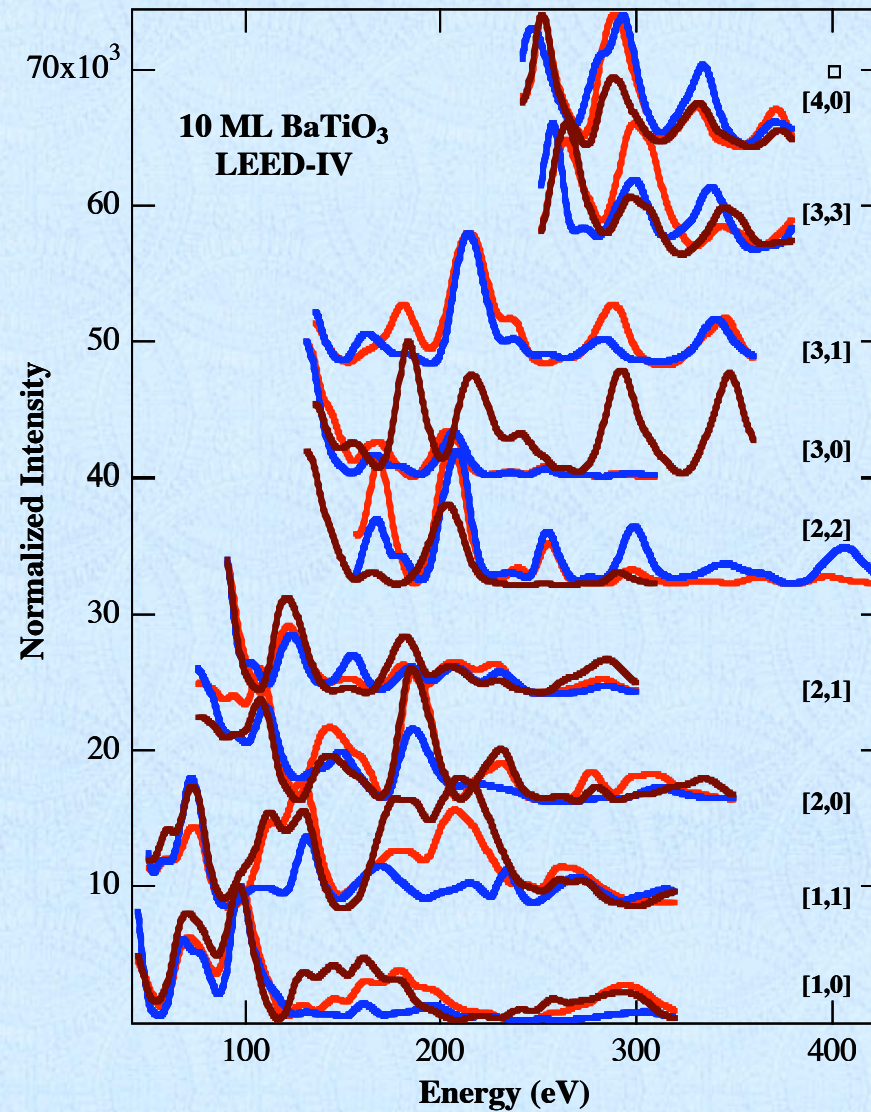
unpolarized

$$R_p = 0.44$$

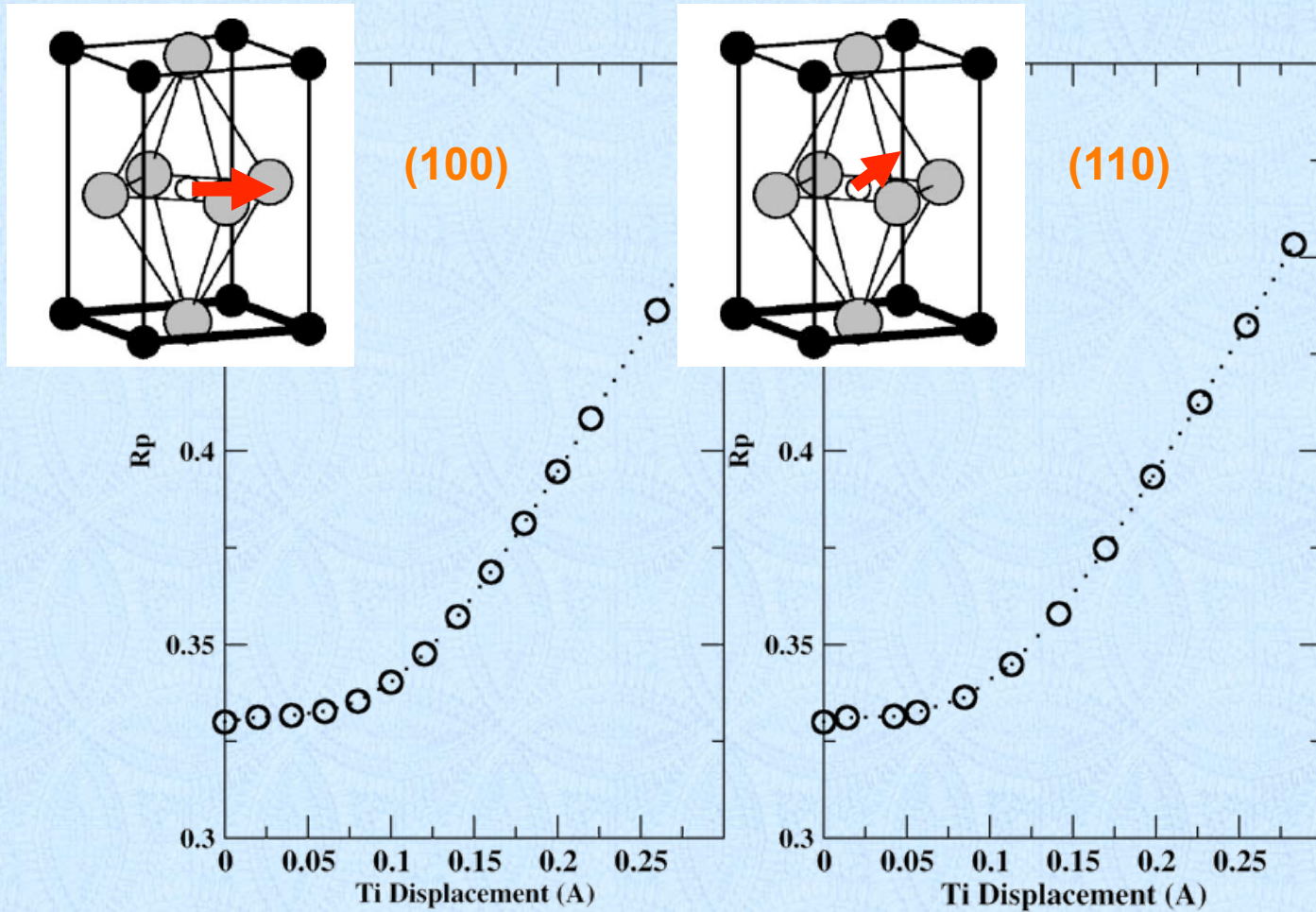
experiment

best model

$$R_p = 0.32$$

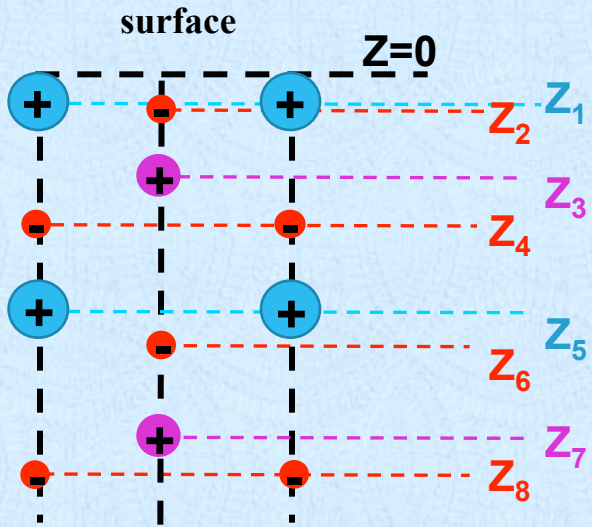


In-Plane Ti Displacement

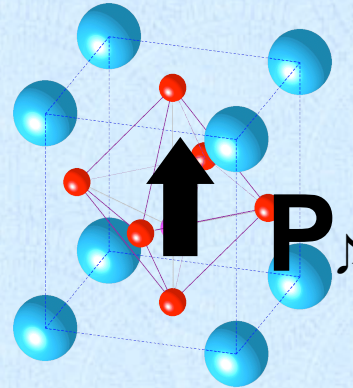


- ❖ best fit with no in-plane Ti displacement
- ❖ possibly large in-plane RMS

10 Layer BaTiO₃ Structure



vertical scale 5x



Polarization

$$\eta(\text{BaO}, \text{TiO}_2) = [\Delta Z(\text{Ba}, \text{Ti}) - \Delta Z(\text{O})] / \text{lattice constant } c$$

Structure

Z ₁	0.0964 ± 0.04 Å
Z ₂	0.1185 ± 0.04 Å
Z ₃	1.9595 ± 0.03 Å
Z ₄	2.1169 ± 0.05 Å
Z ₅	4.1854 ± 0.04 Å
Z ₆	4.3029 ± 0.07 Å
Z ₇	6.1838 ± 0.05 Å
Z ₈	6.3039 ± 0.09 Å

layer	Surface of films	Surface of bulk*		Bulk**
	LEED-IV exp.	DFT theory applied E _{ext}	DFT theory without E _{ext}	Neutron and XRD
1 st , η(BaO)	- 0.0053	- 0.038	+ 0.0151	±0.0240
2 nd , η(TiO ₂)	- 0.0376	- 0.025	- 0.0046	±0.0285
3 rd , η(BaO)	- 0.0281	- 0.022	+ 0.0039	±0.0240
4 th , η(TiO ₂)	- 0.0287			±0.0285

*Meyer and Vanderbilt PRB63, 205426 (2001)

** Harada Acta Cryst. A26, 336 (1970)

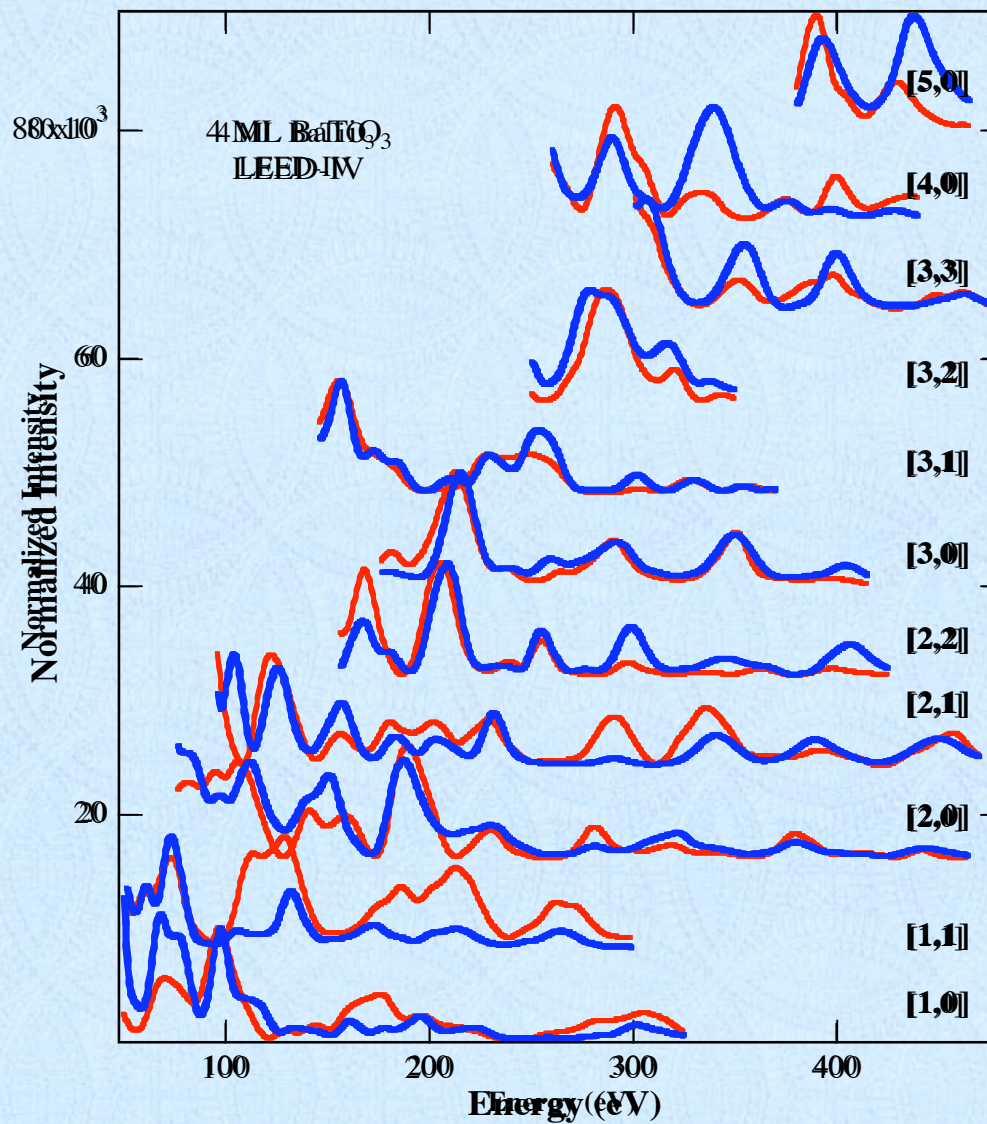
- ❖ upward polarization
- ❖ BaO termination, surface relaxation
- ❖ top dead layer, inside similar to bulk

LEED-IV 4 Layer BaTiO₃ film

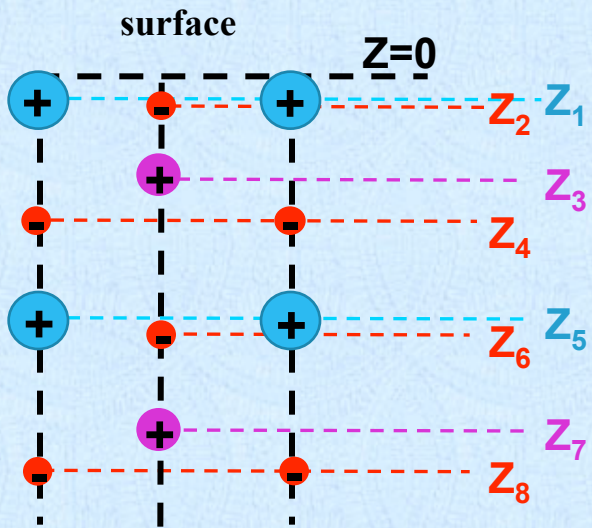
experiment

model

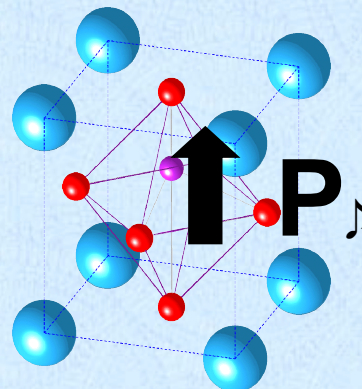
$$R_p = 0.30$$



4 Layer BaTiO₃ Structure



vertical scale 5x



Polarization

$$\eta(\text{BaO}, \text{TiO}_2) = [\Delta Z(\text{Ba}, \text{Ti}) - \Delta Z(\text{O})] / \text{lattice constant } c$$

Z ₁	0.0738 ± 0.03 Å
Z ₂	0.1078 ± 0.04 Å
Z ₃	1.9243 ± 0.02 Å
Z ₄	2.0648 ± 0.05 Å
Z ₅	4.1308 ± 0.04 Å
Z ₆	4.1863 ± 0.07 Å
Z ₇	6.0643 ± 0.04 Å
Z ₈	6.2046 ± 0.10 Å

layer	Surface of films	Surface of bulk*		Bulk**
	LEED-IV exp.	DFT theory applied E _{ext}	DFT theory without E _{ext}	Neutron and XRD
1 st , η(BaO)	- 0.0083	- 0.038	+ 0.0151	±0.0240
2 nd , η(TiO ₂)	- 0.0342	- 0.025	- 0.0046	±0.0285
3 rd , η(BaO)	- 0.0135	- 0.022	+ 0.0039	±0.0240
4 th , η(TiO ₂)	- 0.0341			±0.0285

*Meyer and Vanderbilt PRB63, 205426 (2001)

** Harada Acta Cryst. A26, 336 (1970)

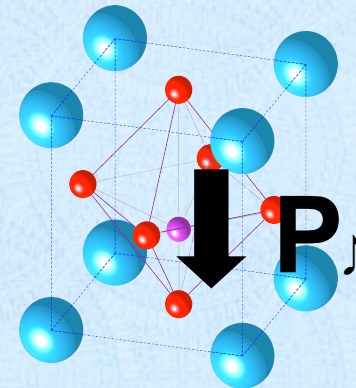
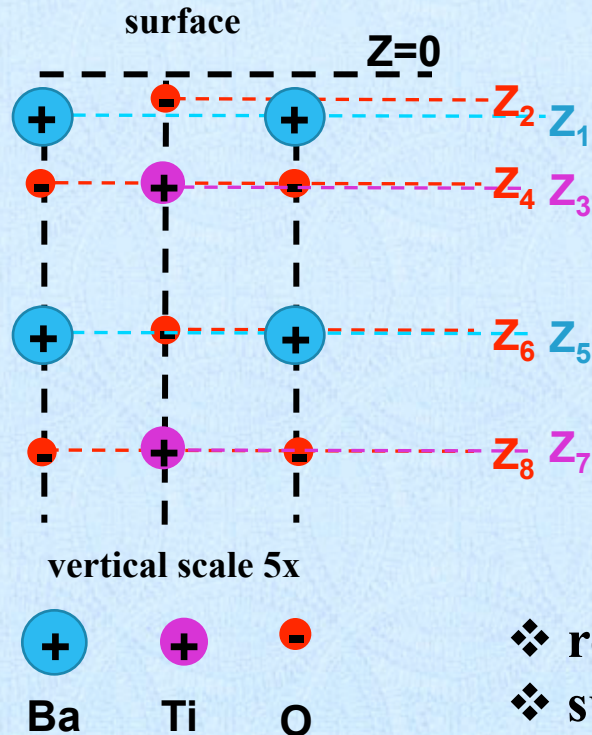
- ❖ upward polarization
- ❖ quite similar to 10 layer film

The Dead Layer

First Principles BaTiO₃ Structure

Meyer and Vanderbilt PRB63, 205426 (2001)

Meyer, Padilla, and Vanderbilt arXiv:Cond-Mat (1999)



- ❖ relaxation
- ❖ surface of unpolarized bulk is polarized inward
- ❖ for BaO termination, 20% bulk corrugation
- ❖ $\downarrow_{\text{relaxation}} + \uparrow_{\text{spontaneous}} = \text{flat surface}$

water

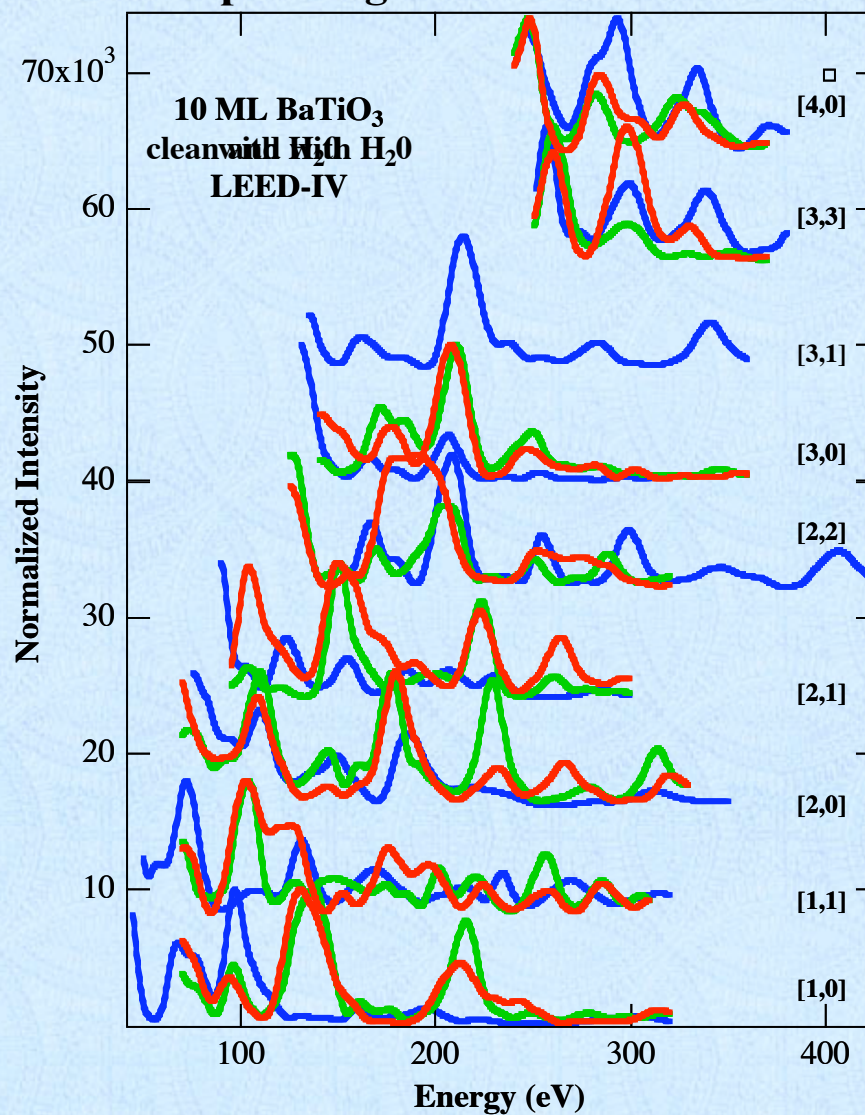
LEED-IV H_2O on 10 Layer $BaTiO_3$ film corresponding to ~60 msec in ambient

clean

with H_2O

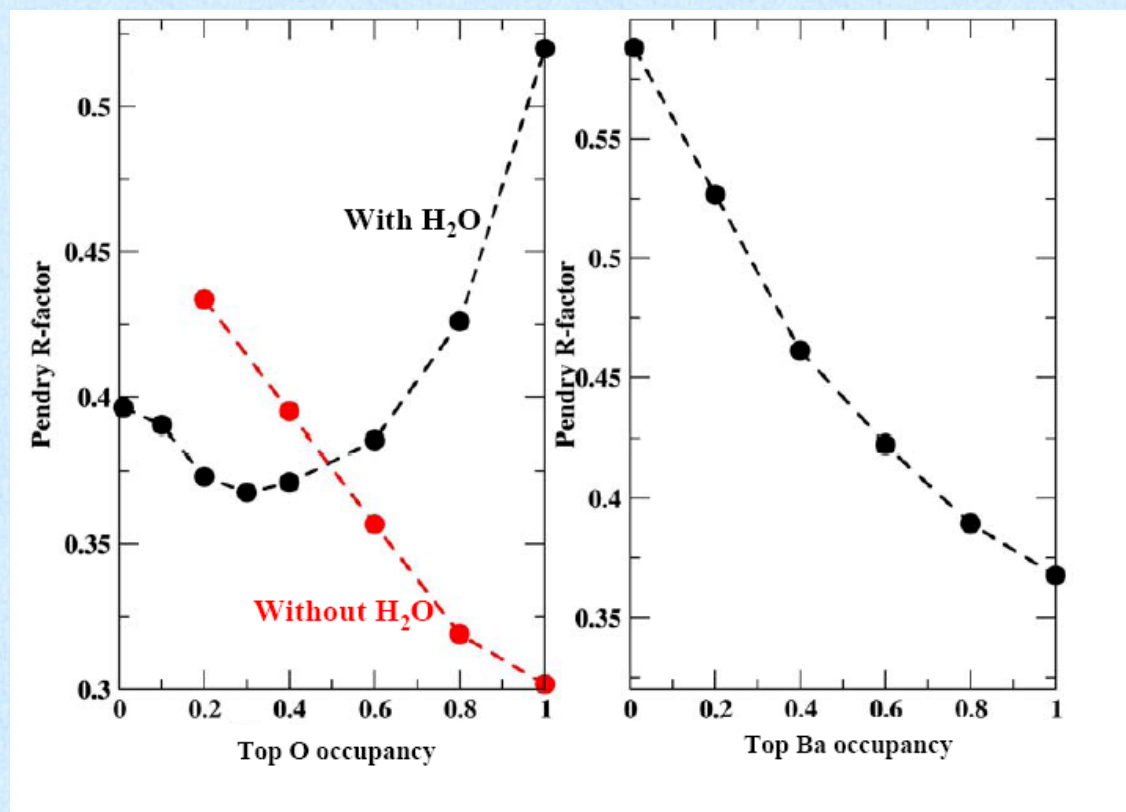
model

$$R_p = 0.39$$



J. Shin, V.B. Nascimento,
G. Geneste, J. Rundgren,
E.W. Plummer,
B. Dkhil, S.V. Kalinin, and
A.P. Baddorf
submitted to PRL 08

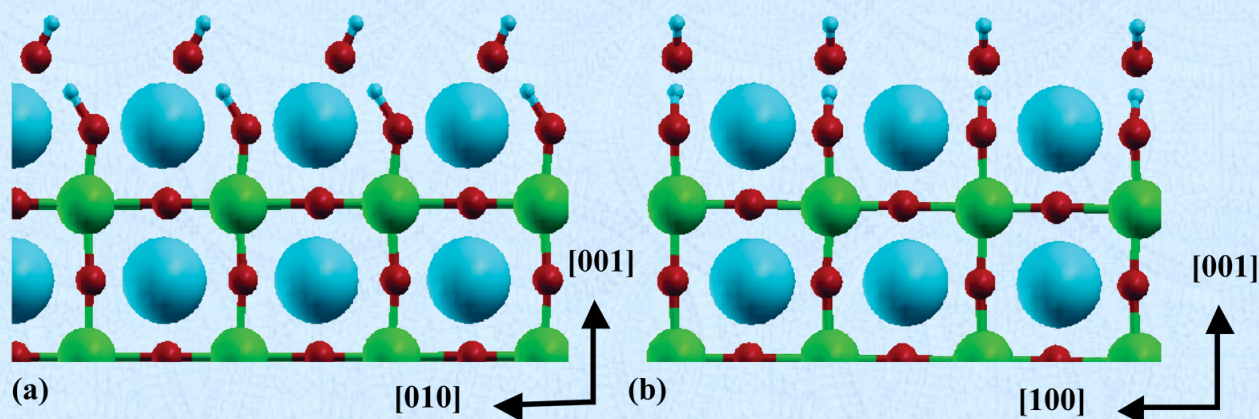
H₂O effect on BaTiO₃ top layer



- ❖ H₂O exposure steals O from top BaTiO₃ layer
- ❖ Ba occupancy unaffected

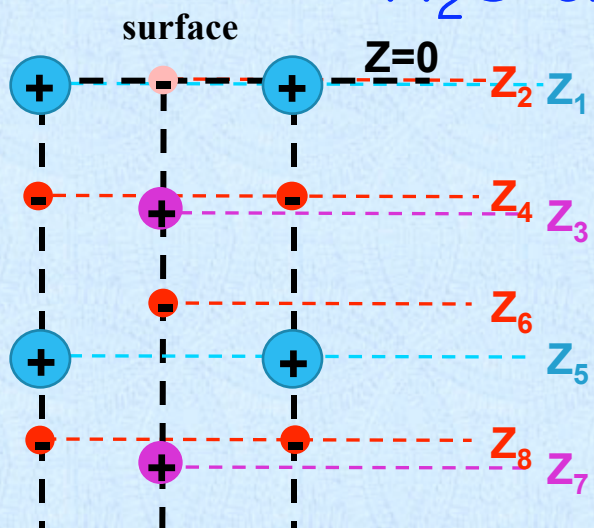
Density Functional Theory $\text{H}_2\text{O}/\text{BaTiO}_3$

G. Geneste and B. Dkhil, Ecole Centrale Paris, France

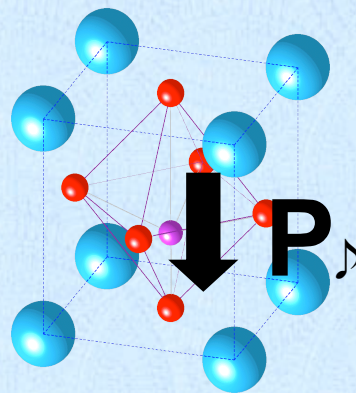


- ❖ solitary H_2O won't chemisorb
- ❖ high exposures lead to dissociation and OH
- ❖ bonding to top layer O in BaO

H₂O exposed BaTiO₃ Structure



vertical scale 5x



Polarization

$$\eta(\text{BaO}, \text{TiO}_2) = [\Delta Z(\text{Ba}, \text{Ti}) - \Delta Z(\text{O})] / \text{lattice constant } c$$

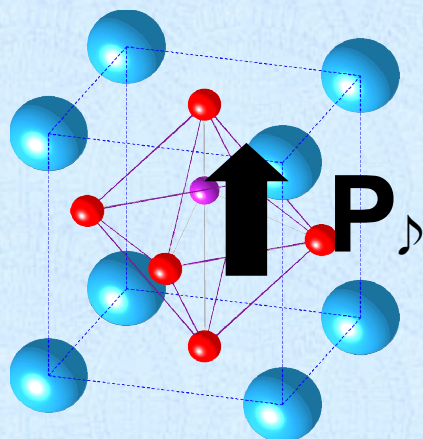
layer	Surface of films	Bulk**
	LEED-IV exp.	Neutron and XRD
1 st , $\eta(\text{BaO})$	+ 0.0050	± 0.0240
2 nd , $\eta(\text{TiO}_2)$	+ 0.0145	± 0.0285
3 rd , $\eta(\text{BaO})$	+ 0.0430	± 0.0240
4 th , $\eta(\text{TiO}_2)$	+ 0.0217	± 0.0285

** Harada Acta Cryst. A26, 336 (1970)

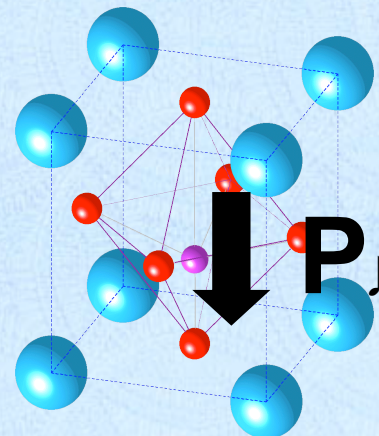
Structure

Z ₁	0.0155 ± 0.03 Å
Z ₂	-0.0053 ± 0.08 Å
Z ₃	2.1136 ± 0.03 Å
Z ₄	2.0527 ± 0.06 Å
Z ₅	4.1100 ± 0.08 Å
Z ₆	3.9299 ± 0.09 Å
Z ₇	6.3236 ± 0.05 Å
Z ₈	6.2327 ± 0.12 Å

- ❖ reversed polarization
- ❖ oxygen vacancies
- ❖ polarization: reduced

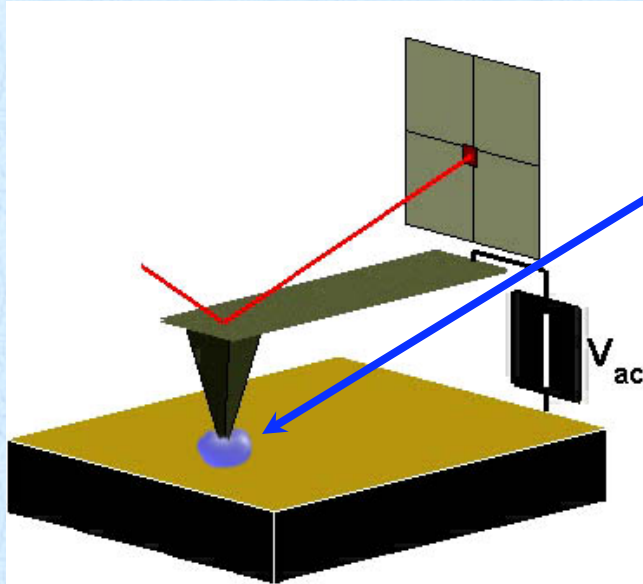


Ultrathin ferroelectricity depends on the surface



Imaging in Air

Almost all PFM studies to date done in ambient



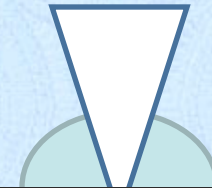
Water meniscus

$\gg 100$ nm

conductivity?

dynamics?

surface chemistry?



Ferroelectric surface

- ❖ electrical boundary conditions are not well defined in air
- ❖ key question: environmental role?

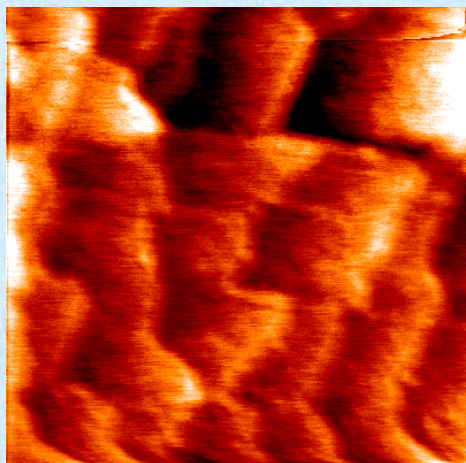


Out-of-Plane UHV PFM

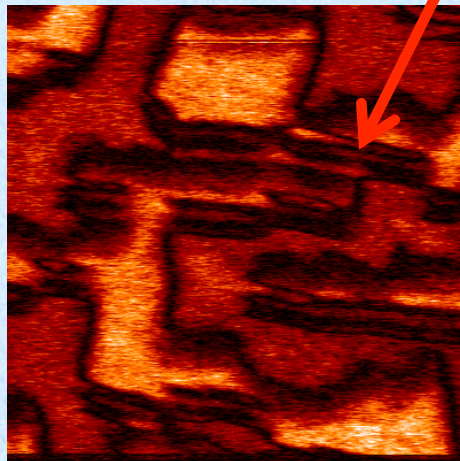
22nm BiFeO₃/SrRuO₃/SrTiO₃(110)

Peter Maksymovych

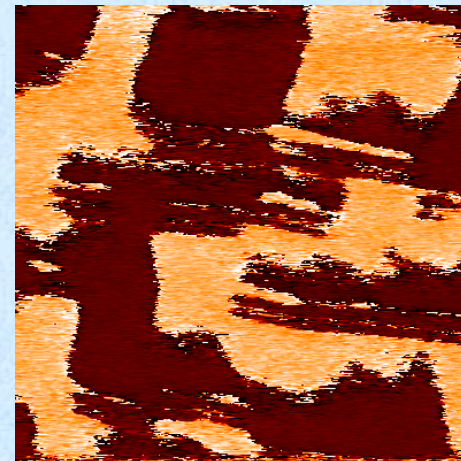
“finger”-like domains



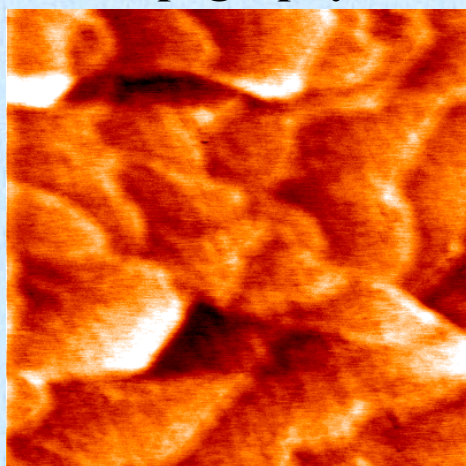
topography



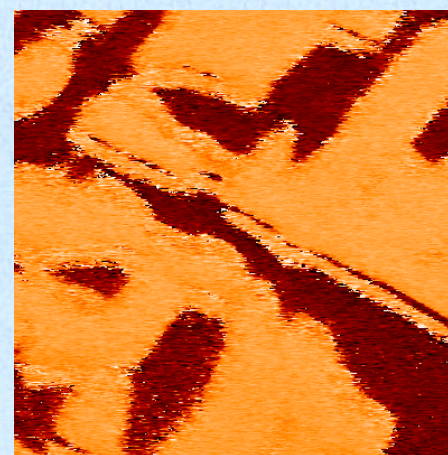
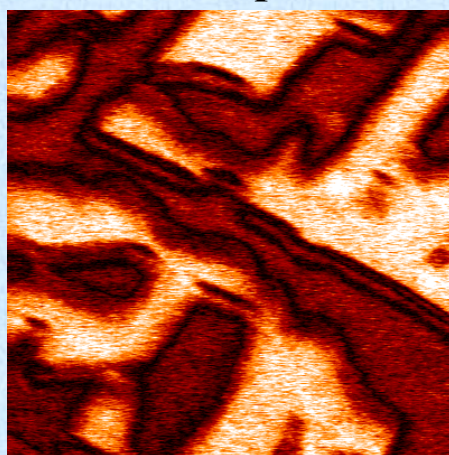
PFM amplitude



PFM phase

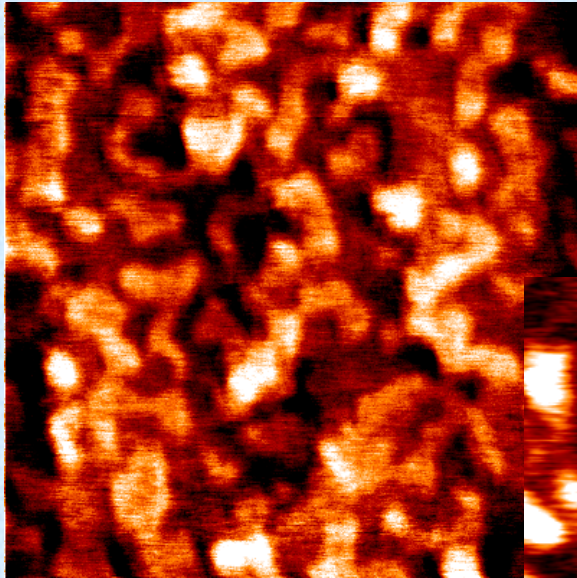


(1x1 μm²)

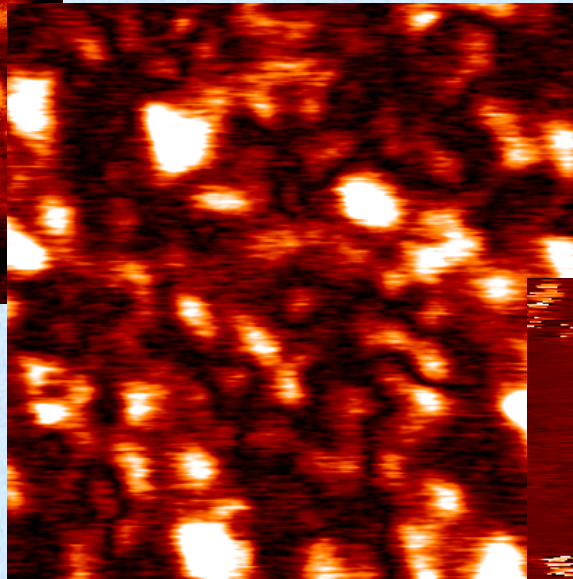


Out-of-Plane UHV PFM

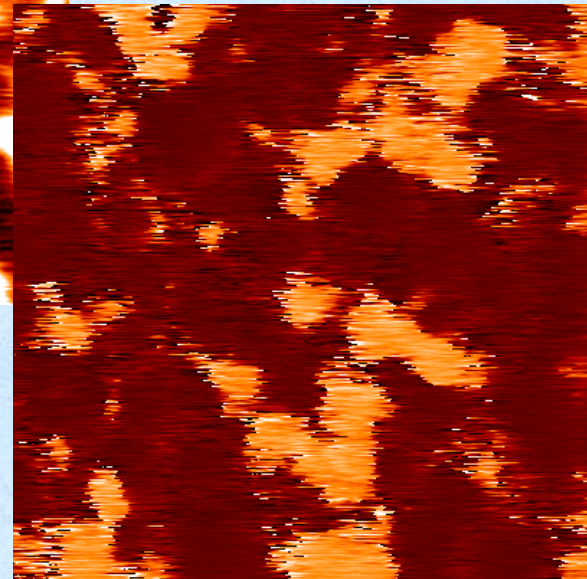
2nm BiFeO₃/SrRuO₃/DyScO₃(110)



topography



amplitude



phase

Out-of-Plane PFM

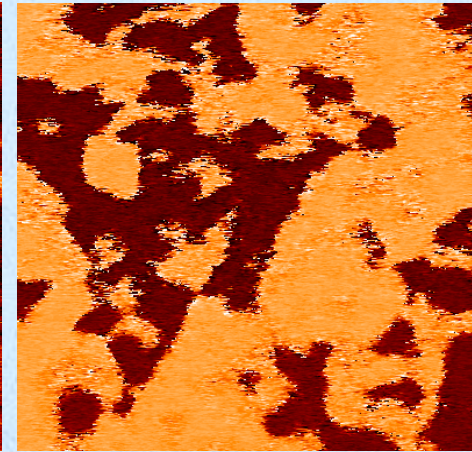
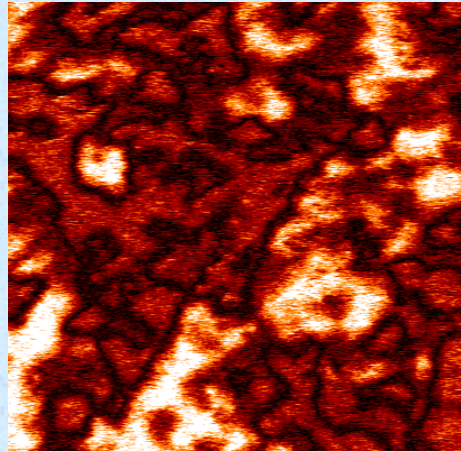
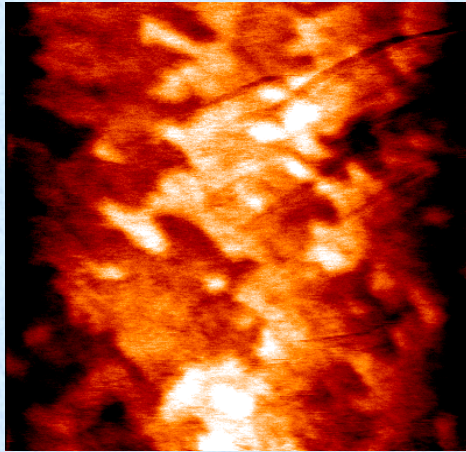
2nm BiFeO₃/SrRuO₃/DyScO₃(110)

Topography

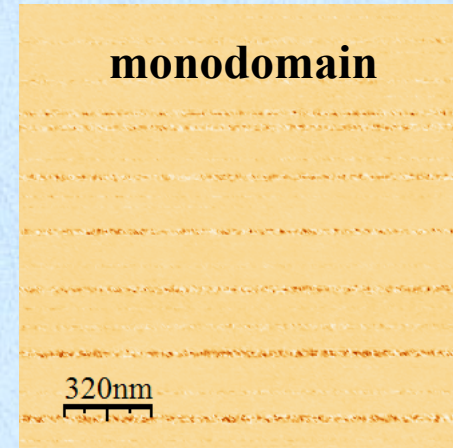
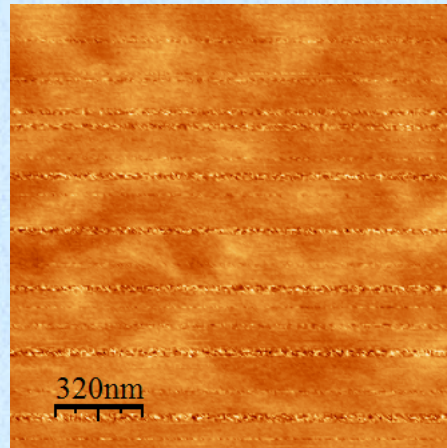
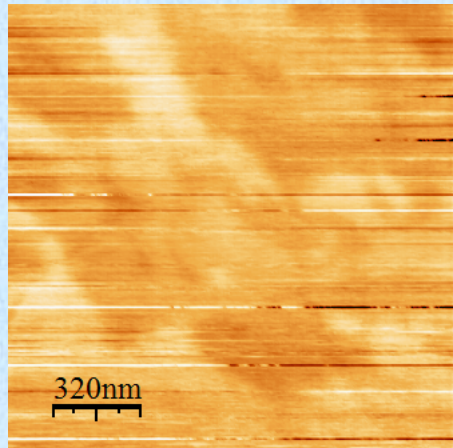
PFM amplitude

PFM phase

UHV



Air

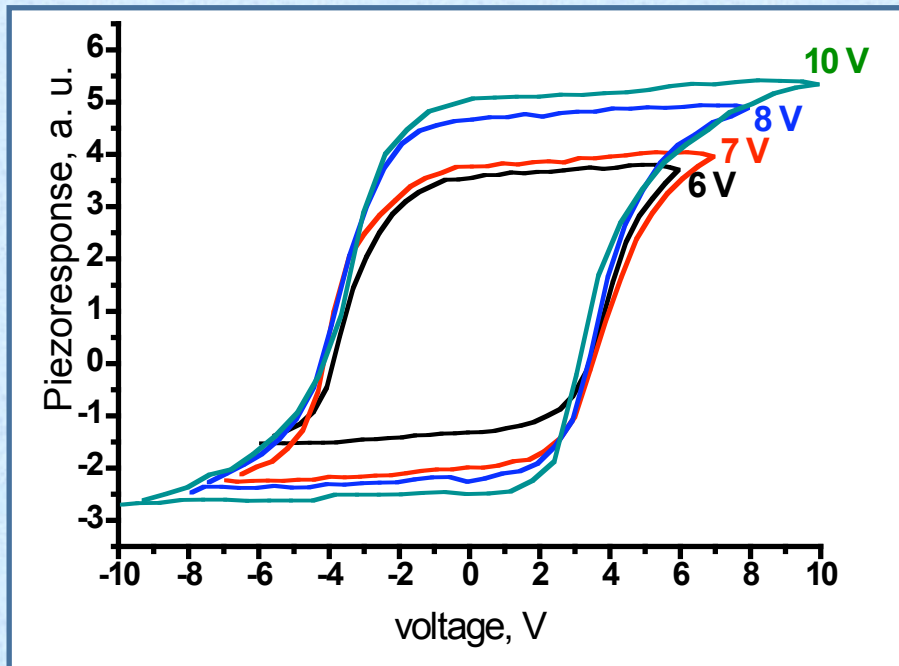


- ❖ surface chemistry dominates
- ❖ control is necessary

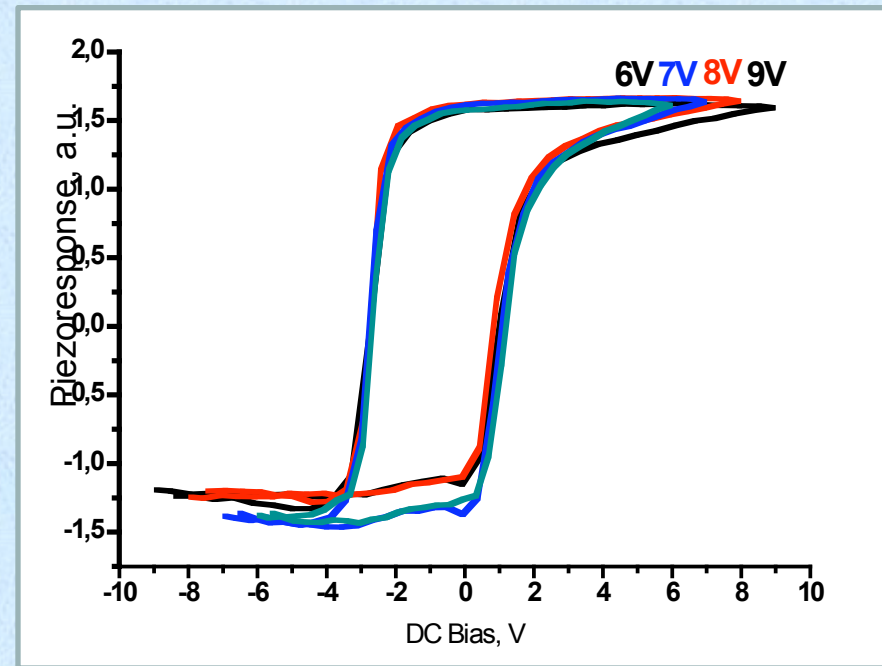
Environment: Thin Films

50 nm BiFeO₃/SrRuO₃/SrTiO₃(110)

Ambient



UHV



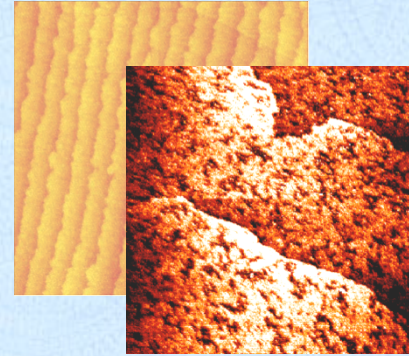
Loops averaged from 100-200 locations
and obtained with the same cantilever in the same chamber on the same day

Qualitatively, vacuum loops have:

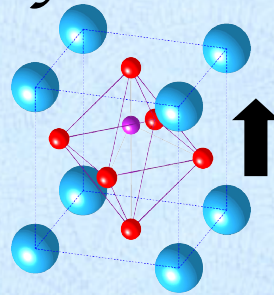
- ❖ lower coercivity
- ❖ lower nucleation bias voltage
- ❖ greater asymmetry

Summary

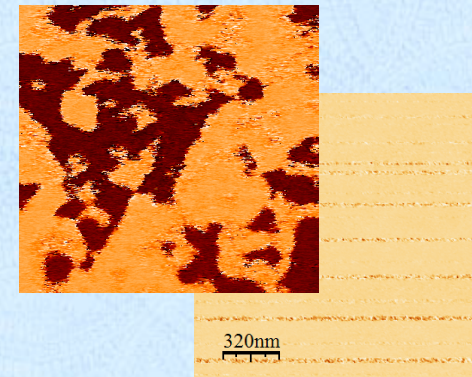
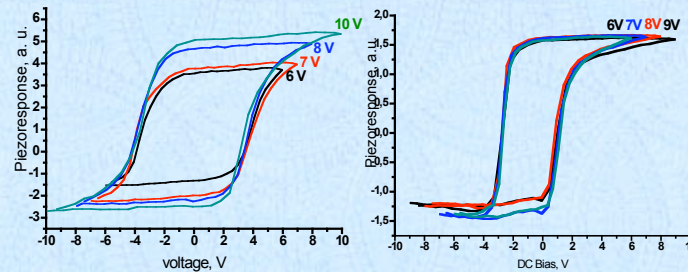
Even "inert" oxides react in air



Ultrathin ferroelectricity depends on the surface



PFM is different in air and vacuum





Center for Nanophase Materials Sciences

www.cnms.ornl.gov

User Center

